The reversible Inlet/Outlet Model

Cumming, P., Kumakura, Y., Schabram, I., & Vernaleken, I.

The specific signal from FDOPA in brain is due to the decarboxylation of the tracer in catecholamine and serotonin fibres, and the retention of [^{18}F]fluorodopamine in synaptic vesicles, mainly in the striatum. However, the interpretation of FDOPA PET scans is complicated due to the accumulation in plasma of the metabolite *O*-methyl-FDOPA (OMFD), which, along with FDOPA, crosses the blood-brain barrier (BBB) by facilitated diffusion mediated by the common carrier for large neutral amino acids. At times after 30 minutes post injection, the plasma OMFD concentration exceeds that of FDOPA in circulation (Figure 1).

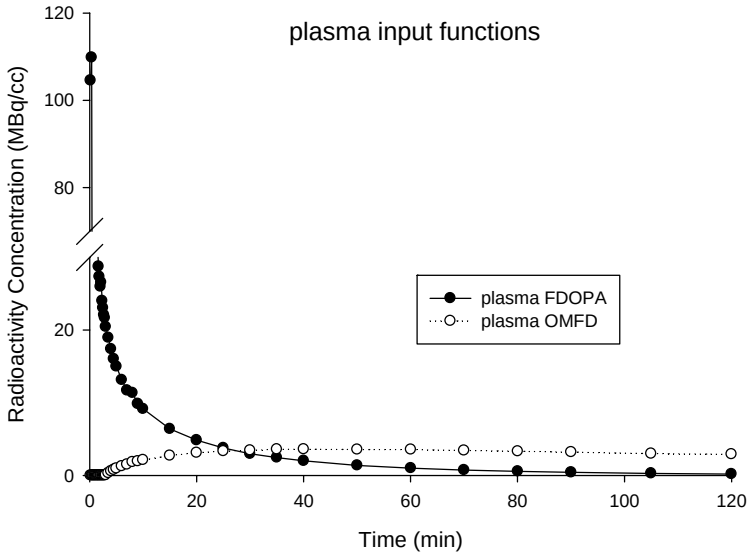

Figure 1. An example of FDOPA and OMFD plasma input functions obtained from a FDOPA PET study for a 52 year old normal control subject.

Interference from OMFD in brain images can be reduced by pharmacological blockade of the enzyme catechol-*O*-methyltransferase (Cumming et al., 1987; Léger et al., 1998). More frequently, the net influx of FDOPA to brain (K_{in}^{app}; ml g^{-1} min^{-1}) is approximated by subtraction of the entire radioactivity measured in cerebellum, or

other reference region nearly devoid of DOPA decarboxylase activity, followed by application of a linear graphical analysis relative to the metabolite-corrected arterial input for FDOPA (Martin et al., 1989); the net influx K_{in}^{app} is a macroparameter, defined in terms of the unidirectional blood-brain clearance of FDOPA (K_1^D; ml g^{-1}), the fractional rate constant for diffusion of FDOPA in brain back to circulation (k_2^D; min^{-1}), and the relative activity of DOPA decarboxylase in brain (k_3^D; min^{-1}), i.e. (K_1^D x k_3^D)/(k_2^D + k_3^D). This model is illustrated in Figure 2A. However, the linear graphical approach suffers from over-subtraction of brain FDOPA, resulting in undefined [^{18}F]fluorodopamine formation in striatum during the first 10-20 minutes of the dynamic PET recording, and furthermore fails to accommodate the diffusion from brain of deaminated [^{18}F]fluorodopamine metabolites, which becomes very substantial within an hour or tracer injection (Cumming et al., 2001).

A more physiologically relevant analysis entails a constrained compartmental model, which affords the estimation of the relative activity of DOPA decarboxylase in living brain (k_3; min^{-1}; Gjedde et al., 1991; Huang et al., 1991). This model implicitly entails at least five kinetic parameters, i.e. the unidirectional blood-brain clearances of FDOPA (K_1^D) and OMFD (K_1^M), the fractional rate constants for the diffusion from brain of FDOPA (k_2^D) and OMFD (k_2^M), and the relative activity of DOPA decarboxylase (k_3^D). As implemented by Huang et al., (1991), the model also accommodates a rate constant for the clearance from brain of [^{18}F]fluorodopamine together with its deaminated metabolites (Figure 2). This clearly over-specified model is simplified through the use of two physiologically-justified constraints: First, the blood brain permeabilities of OMFD and FDOPA are held to have a constant ratio in all brain regions (q; K_1^M/K_1^D); the magnitude of q has been explicitly measured once in rat ($q = 2.2$; Reith et al., 1990), and in

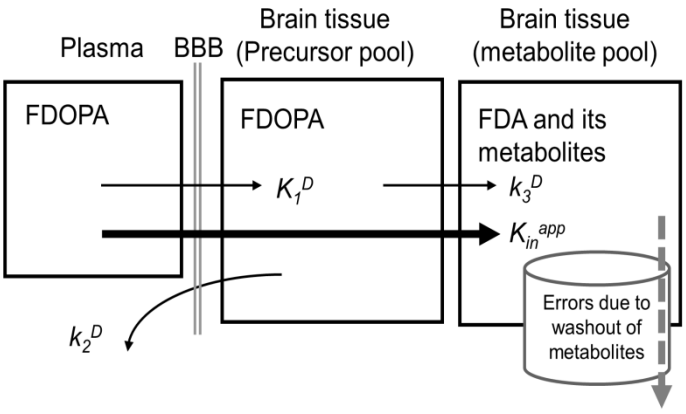

(A) Conventional irreversible model

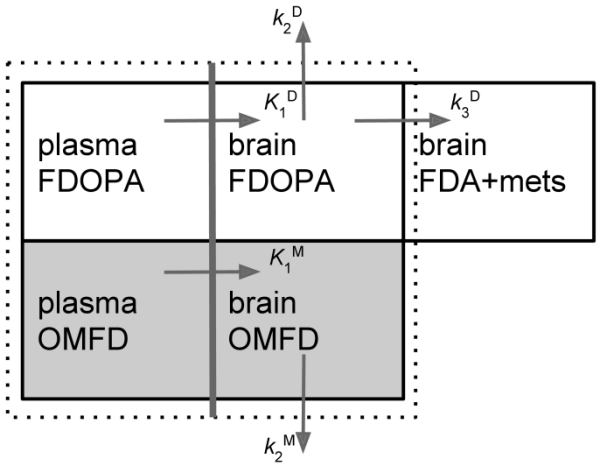

(B) Mathematical OMFD subtraction

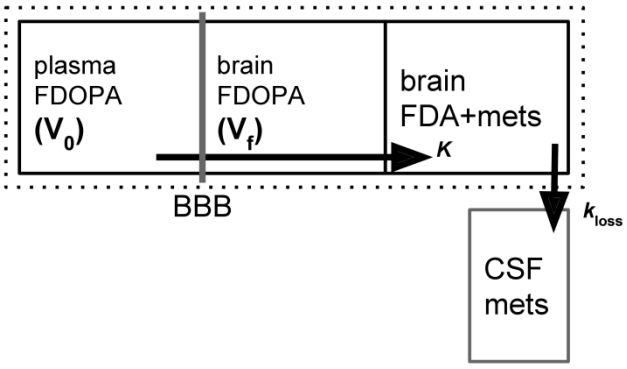

(C) Reversible inlet-and-oulet model

Figure 2. The several approaches to kinetic modelling of FDOPA. (A) The conventional linear graphic analysis, with (over)-subtraction of the entire cerebellum TAC so as to remove the contribution of brain OMFD. The net influx Kinapp is a macro-parameter defined by the unidirectional blood-brain clearance (K_1^D), the diffusion of FDOPA in brain back to circulation (k_2^D), and the irreversible trapping of [^{18}F]fluorodopamine in brain (k_3^D), neglecting in most applications the real and progressive loss of

decarboxylated and deaminated metabolites. (B) The compartmental model employing a dual input function, with constraints to reduce the number of parameters. In the IOM, the cerebellum TAC for OMFD is calculated and subtracted from the entire dynamic brain volume, in order to isolate the decarboxylation pathway. (C) The IOM is then used to estimate the intrinsic clearance of FDOPA to brain (K), and the washout rate constant (k_{loss}). Figure modified from Kumakura and Cumming (2009).

three human PET studies: (q = 0.7 (normals) or 1.0 (Parkinson's disease) Dhawan et al., 1996); q=1.1 (Wahl and Nahmias, 1996), and q = 1.7 (Huang et al., 1991), giving a mean value of q=1.5 (see Cumming and Gjedde, 1998). The claim that K_1^M/K_1^D exceeds unity has face validity, given the general relationship between the octanol/water partition coefficient of LNAAs and their transport kinetics (Smith et al., 1987), and the substantially different retention times of OMFD and DOPA by reverse phase liquid chromatography. However, we have shown that the estimation of the parameter of main interest is not highly sensitive to the magnitude of q, in the range from 1 – 2 (Figure 3).

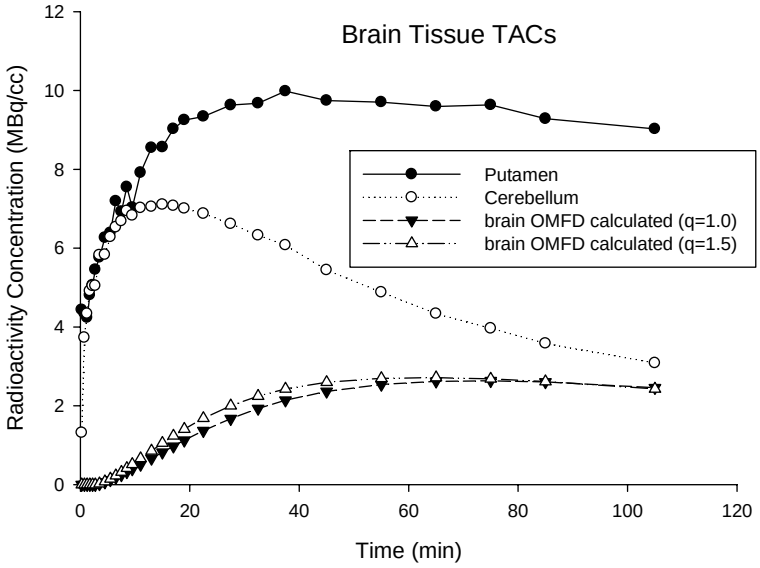

Figure 3. Calculated brain OMFD TACs obtained using the OMFD arterial input function and two different magnitudes of q (q=1.0 and 1.5), together with total PET TACs of putamen and cerebellum obtained from the same FDOPA experiment are shown in Figure 1. The dual input constrained fitting of cerebellum gave K_1^D=0.041 ml g^{-1} min^{-1}, and k_2^D=0.057 min^{-1}). The calculated brain OMFD curves differ only with respect to the curvature of the middle phase (15-60 min), and converge perfectly towards the end of the 120 minute recordings. In practice, this difference has little effect on the calculation

of the magnitude of the three IOM parameters (K, V_d and k_{loss}).

The second constraint used in the compartmental analysis of FDOPA is to assume that the equilibrium distribution volumes for FDOPA (K_1^D/k_2^D) and OMFD (K_1^M/k_2^M) are identical throughout brain. This is to be expected for any amino acid with facilitated diffusion across the blood-brain barrier, and a large body of evidence indicates that the common distribution volume is close to that expected from the water content of brain divided by that of blood. i.e. approximately 0.75 ml g^{-1}.

The constrained compartmental model for FDOPA is evaluated in two steps. First, the common partition volume for FDOPA and OMFD is calculated in cerebellum (dotted box in Figure 2B), where the activity of DOPA decarboxylase is expected to be close to zero. Knowing the arterial inputs for FDOPA and OMFD during 60 minutes, the common distribution volume is calculated as the sum of the OMFD content in cerebellum,

$$M^M(t) = K_1^M \mathrm{e}^{-k_2^M(t)} \otimes C_p^M(t) + V_0 C_p^M(t) \quad (1)$$

And the FDOPA content in cerebellum,

$$M^D(t) = K_1^D \mathrm{e}^{-k_2^D(t)} \otimes C_p^D(t) + V_0 C_p^D(t) \quad (2)$$

i.e. the sum $M^D(t) + M^M(t)$ with the constraints as noted above: $q = K_1^M / K_1^D = 1.5$, and a common equilibrium distribution volume for the two amino acids in brain, $V_e = K_1^D/k_2^D = K_1^M/k_2^M$. These constraints reduced the number of unknown parameters to two, K_1^D, V_e, when V_0, the plasma volume in brain, is assumed to be constant, i.e. 0.05 ml g^{-1}.

As noted above, the net influx of FDOPA from plasma to brain by facilitated diffusion at the BBB and metabolic trapping is susceptible to the progressive loss of the decarboxylated metabolites. While [^{18}F]fluorodopamine is not itself diffusible, it is deaminated by monoamine oxidase, yielding [^{18}F]fluoro-DOPAC, which is a substrate for COMT in brain, yielding [^{18}F]fluoro-HVA. Both of these acidic metabolites diffuse across

the BBB (Cumming et al., 1994), leading to a substantial loss of trapped signal in the course of prolonged PET recordings. This phenomenon can be used to advantage in steady-state analyses of FDOPA PET recordings. We have developed the inlet-outlet model (IOM) for calculating kinetic rate constants for both the intrinsic FDOPA transfer corrected for loss (K) and the elimination of decarboxylated metabolites from brain (k_{loss}), by considering [^{18}F]fluorodopamine together with its deaminated metabolites to occupy a single diffusible pool in brain.

The IOM model is evaluated in two stages. First, the brain time-activity curve for OMFD in cerebellum is calculated with the constrained compartmental model, using equations 1 and 2, above. The entire dynamic PET recording is then subtracted frame-wise by the calculated brain OMFD curve (Kumakura et al. 2005), which isolates the brain radioactivities due to FDOPA, [^{18}F]fluorodopamine, and its deaminated metabolites. We next evaluate the local magnitude of FDOPA-K, which disregards the (FDOPA) precursor pool in brain. Then, the brain concentration $M_m(t)$, i.e. [^{18}F]fluorodopamine and its deaminated metabolites, can be expressed as a first order differential equation Eq.(3), involving the arterial plasma FDOPA concentration $C_p(t)$, as a function of circulation time (Kumakura et al. 2006).

$$\frac{dM_m(t)}{dt} = KC_p(t) - k_{loss}M_m(t) \tag{3}$$

An integration operation yields Eq.(4).

$$M_m(t) = K\int_0^t C_p(\tau)d\tau - k_{loss}\int_0^t M_m(\tau)d\tau \tag{4}$$

Assuming that the distribution volume of the precursor pool (V_f) approaches a constant after a certain period of time (10-20 min after the dose injection), and given an effective plasma volume in brain (V_0), the total mass of the tracer in the VOI after subtraction of OMFD, $M(t)$ can be expressed by Eq.(5).

$$M(t) = M_m(t) + (V_f + V_0)C_p(t) \tag{5}$$

Isolating $M_m(t)$ to the left side gives Eq.(6)

$$M_m(t) = M(t) - (V_f + V_0)C_p(t) \tag{6}$$

Substituting the right side of Eq.(6) for two functions of $M_m(t)$ on both sides of Eq.(4) gives Eq.(7)

$$M(t) - (V_f + V_0)C_p(t) = K\int_0^t C_p(\tau)d\tau - k_{loss}\int_0^t \{M(\tau) - (V_f + V_0)C_p(\tau)\}d\tau \tag{7}$$

which is the same as Eq.(8), and after collecting like terms as Eq.(9).

$$M(t) = K\int_0^t C_p(\tau)d\tau - k_{loss}\int_0^t M(\tau)d\tau + k_{loss}(V_f + V_0)\int_0^t C_p(\tau)d\tau + (V_f + V_0)C_p(t) \tag{8}$$

$$M(t) = \{K + k_{loss}(V_f + V_0)\}\int_0^t C_p(\tau)d\tau - k_{loss}\int_0^t M(\tau)d\tau + (V_f + V_0)C_p(t) \tag{9}$$

Dividing both sides of Eq.(9) by k_{loss}, and placing the terms with kinetic coefficients to be estimated on the right side gives Eq. (10).

$$\int_0^t M(\tau)d\tau = \{EDV + (V_f + V_0)\}\int_0^t C_p(\tau)d\tau - \frac{M(t)}{k_{loss}} + \frac{(V_f + V_0)}{k_{loss}}C_p(t) \tag{10}$$

By applying multiple time points of OMFD-subtracted brain TACs to this linearized solution Eq.(8), a set of system equations enables calculation for the magnitudes of the three coefficients (macroparameters): P(1)=V_d =$\{EDV+(V_f + V_0)\}$, P(2)=$1/k_{loss}$, P(3)=$(V_f + V_0)/k_{loss}$. Thus, the first kinetic parameter V_d equals P(1), the second parameter k_{loss} is calculated as the reciprocal of P(2), and the third parameter K is calculated as EDV multiplied by k_{loss}, all the three macroparameters (P(1), P(2) and P(3)). In order to avoid negative kinetic estimates, a function in Optimization Toolbox of MATLAB (The MathWorks, Inc., Natick, Mass, USA.) for solving constrained linear

least-squares problems is useful.

References:

Cumming P, Boyes BE, Martin WR, Adam M, Ruth TJ, McGeer EG. (1987) Altered metabolism of [18F]-6-fluorodopa in the hooded rat following inhibition of catechol-O-methyltransferase with U-0521. Biochem Pharmacol. 36(15):2527-31.

Cumming P, Kuwabara H, Gjedde A. (1994) A kinetic analysis of 6-[18F]fluoro-L-dihydroxyphenylalanine metabolism in the rat. J Neurochem. 63(5):1675-82.

Cumming, P, and Gjedde, A. (1998) Compartmental analysis of dopa decarboxylation in living brain from dynamic positron emission tomograms. Synapse 29, 37-61.

Cumming P, Munk OL, Doudet D. (2001) Loss of metabolites from monkey striatum during PET with FDOPA. Synapse. 41(3):212-8.

Dhawan V, Ishikawa T, Patlak C, Chaly T, Robeson W, Belakhlef A, Margouleff C, Mandel F, Eidelberg D. (1996) Combined FDOPA and 3OMFD PET studies in Parkinson's disease. J Nucl Med. 37(2):209-16.

Gjedde A, Reith J, Dyve S, Léger G, Guttman M, Diksic M, Evans A, Kuwabara H. (1991) Dopa decarboxylase activity of the living human brain. Proc Natl Acad Sci U S A. 88(7):2721-5.

Huang SC, Yu DC, Barrio JR, Grafton S, Melega WP, Hoffman JM, Satyamurthy N, Mazziotta JC, Phelps ME. (1991) Kinetics and modeling of L-6-[18F]fluoro-dopa in human positron emission tomographic studies. J Cereb Blood Flow Metab. 11(6):898-913.

Kumakura Y, Vernaleken I, Gründer G, Bartenstein P, Gjedde A, and Cumming P. (2005) PET studies of net blood-brain clearance of FDOPA to human brain: Age-dependent decline of [^{18}F]fluorodopamine storage capacity. J Cereb Blood Flow Metab. 25, 807-19.

Kumakura Y, Gjedde A, Danielsen E, Christensen S, and Cumming P. (2006) Dopamine storage capacity in caudate and putamen of patients with early Parkinson's disease; correlation with asymmetry of motor symptoms. J Cereb Blood Flow Metab. 26:358-70.
Kumakura et al., 2006.

Kumakura Y, Cumming P. (2009) PET studies of cerebral levodopa metabolism; A review of clinical findings and modeling approaches [Invited review] Neuroscientist. 15(6), 635-50.

Léger G, Gjedde A, Kuwabara H, Guttman M, Cumming P. (1998) Effect of catechol-O-methyltransferase inhibition on brain uptake of [18F]fluorodopa: implications for compartmental modelling and clinical usefulness. Synapse. 30(4):351-61.

Martin WR, Palmer MR, Patlak CS, Calne DB. (1989) Nigrostriatal function in humans studied with positron emission tomography. Ann Neurol 26:535–42.

Reith J, Dyve S, Kuwabara H, Guttman M, Diksic M, Gjedde A. (1990) Blood-brain transfer and metabolism of 6-[18F]fluoro-L-dopa in rat. J Cereb Blood Flow Metab. 10(5):707-19.

Smith QR, Momma S, Aoyagi M, Rapoport SI. (1987) Kinetics of neutral amino acid transport across the blood-brain barrier. J Neurochem. 49(5):1651-8.

Wahl L, Nahmias C. (1996) Modeling of fluorine-18-6-fluoro-L-Dopa in humans. J Nucl Med. 37(3):432-7.